Chapter 3

Results

Invasion Phenotyping

A total of 46 Peruvian *P. falciparum* samples were thawed and cultured *in* vitro. All samples had been isolated from patients in the Zungoracocha community near Iquitos, Peru, and had been cultured for between 1 week and 3 months at the Universidad Nacional Amazonia de Peruana. All samples were cultured for a minimum of six weeks after which, if no growth occurred, the sample was recorded as negative for growth.

Eleven isolates grew successfully (24%). Of these, ten isolates underwent phenotyping, genotyping and RNA extraction (Table 3.1). 9050 was genotyped and then frozen again, but as it could not be re-cultured successfully no phenotyping or RNA extraction was performed.

Sample	Phenotyped?	Sequenced?	RNA Extracted?	Gametocytogenesis?
278	Yes	Yes	Yes	Yes
788	Yes	Yes	Yes	No
3106	Yes	Yes	Yes	No
3135	Yes	Yes	Yes	No
3541	Yes	Yes	Yes	No
3769	Yes	Yes	Yes	No
5802	Yes	Yes	Yes	Yes
5809	Yes	Yes	Yes	Yes
5814	Yes	Yes	Yes	Yes
6390	Yes	Yes	Yes	Yes
9050	No	Yes	No	Yes

Table 3.1. The 11 isolates that were cultured successfully.

From the 35 samples that could not be cultured, three strains (including 9050) were successfully thawed and asexual parasites were observed in the first few days, but within two weeks the only parasites present were in the sexual gametocyte stage. By four weeks, all gametocytes had died. No parasites were observed in the other 32 samples at any point (Appendix Table A1).

In the eleven isolates that grew, parasites were observed no later than the second day of culture. Multiplication rates were very variable, with samples taking up to four weeks to reach a parasitaemia that was sufficiently high and synchronous to perform phenotyping assays. The time taken for cultures to reach sufficient parasitaemia was further elongated by the requirement of large volumes of culture for DNA and RNA extraction and for freezing

aliquots of each isolate. Samples with low multiplication rates also had a tendency to produce gametocytes in culture.

From the eleven samples that were cultured successfully, invasion assays were carried out on ten samples to assess the parasites' ability to invade receptor-depleted erythrocytes (9050 could not be re-cultured and was therefore not phenotyped, as noted above). Phenotyping was carried out using a two-colour flow cytometry based assay (Theron et al. 2010; see Chapter 2 "Materials and Methods"). This approach uses erythrocytes that have been labelled with an intracellular fluorescent dye (DDAO-SE) and then treated with one of several different enzymes that remove a subset of receptors utilised in parasite invasion from the surface of labelled erythrocytes. The labelled erythrocytes are mixed in equal volume with unlabelled *P. falciparum* infected erythrocytes and cultured for 48 hours before parasite density is measured using fluorescent DNA dyes, either SYBR Green I or Hoechst 33342. Dot plots were produced by a BD LSRII flow cytometer and from these parasitaemias in labelled and unlabelled erythrocytes were calculated (Fig. 3.1). Fluorescence labelling was confirmed by confocal microscopy (Fig. 3.2).

Nine samples were phenotyped using Hoechst 33342 to stain the parasitic DNA and one using SYBR Green I. Two isolates (3135 and 3769) required post-invasion trypsin treatment in order to be phenotyped because of the presence of a secondary population on dot-plots (See Chapter 3 "Results: Extra Populations"). To maintain consistency, all nine isolates were phenotyped using the post-invasion trypsin step, although seven of these samples were also phenotyped without post-invasion trypsin treatment (Appendix Figs. A1 & A2). One sample (278) could not be re-cultured after being frozen and was therefore phenotyped using SYBR Green I as a DNA dye and did not undergo post-invasion trypsin treatment. All isolates were phenotyped on two independent occasions and each assay condition was performed in triplicate in each experiment and the mean parasitaemias for each enzyme treatment were determined (Fig. 3.3).

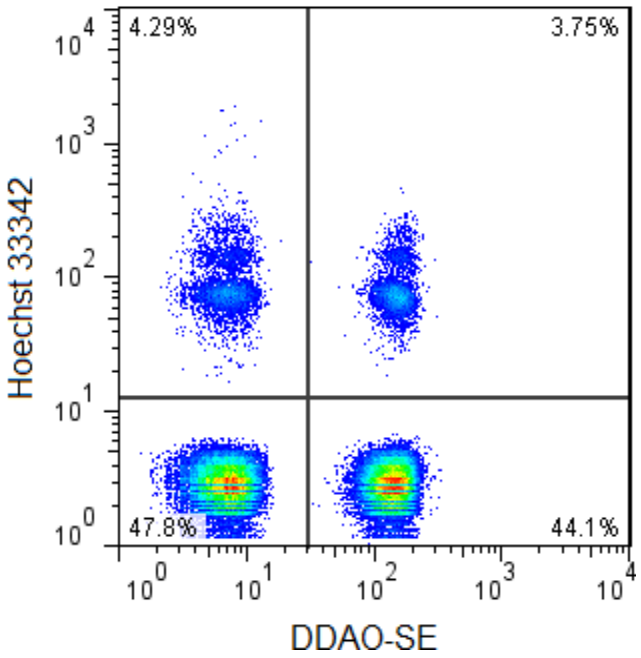

Fig. 3.1. Dot plot of an invasion assay. The plot indicates invasion of strain 3D7 into untreated erythrocytes. The x-axis is DDAO-SE cell labelling and the y-axis is Hoechst 33342 parasite DNA labelling. The four populations (clockwise from bottom right) are: target uninfected cells, donor uninfected cells, donor infected cells and target infected cells. Target infected cells (top right), is the population that varies with enzyme treatment and determines the phenotype.

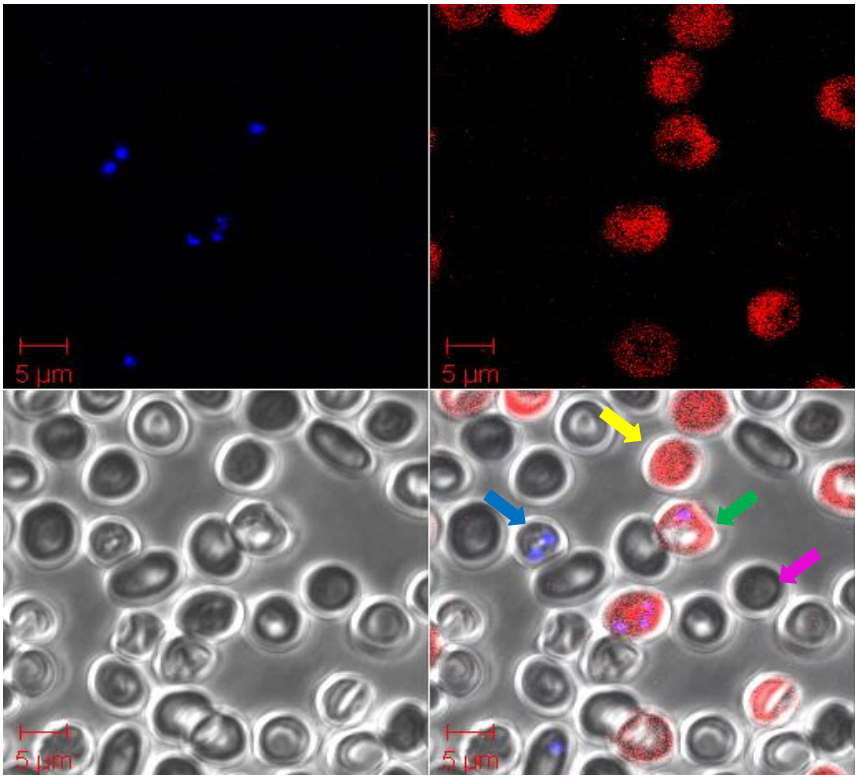

Fig. 3.2. Confocal fluorescence microscopy of erythrocytes from the same well as the dot plot above. The four panels are of the same field with different fluorescence excitation. Clockwise (from bottom right): All fields merged; brightfield; violet laser – Hoechst 33342 parasite labelling; red laser – DDAO-SE cell labelling. Blue arrow: infected, donor erythrocyte. Yellow arrow: uninfected, target erythrocyte. Green arrow: infected, target erythrocyte. Pink arrow: uninfected, donor erythrocyte.

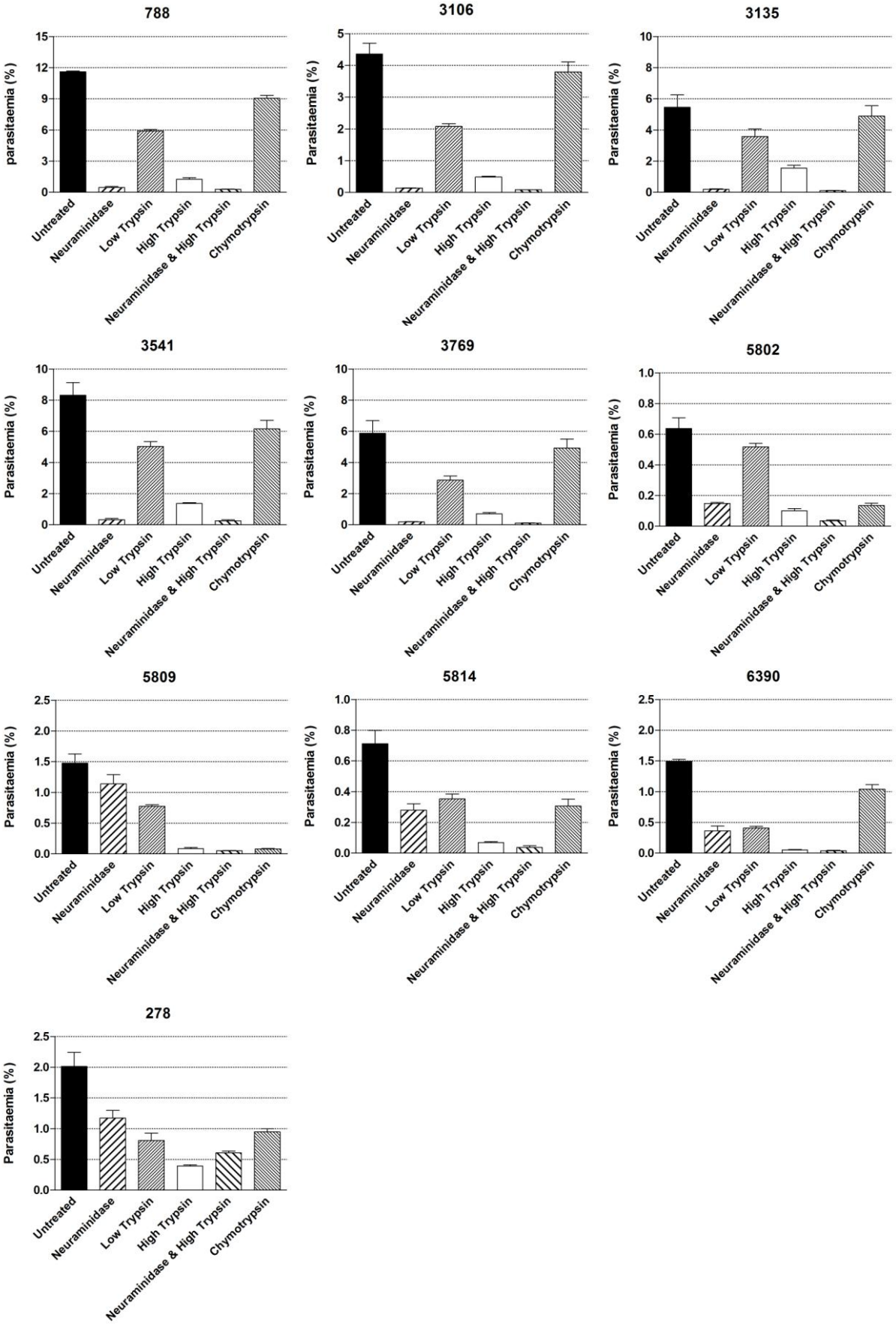

Fig. 3.3. Parasitaemia bar graphs of each phenotyping invasion assay. The bars represent the mean parasitaemia calculated from two experiments of three replicates. Error bars are SEMs.

From the parasitaemias measured in labelled erythrocytes (Fig. 3.3), mean invasion efficiencies for all 10 Peruvian isolates were calculated by expressing the parasitaemia in labelled erythrocytes that underwent each enzyme treatment as a percentage of the parasitaemia in labelled untreated erythrocytes (Fig. 3.4). For example, if an enzyme treatment causes a 20% decrease in parasitaemia with respect to untreated erythrocytes, the invasion efficiency would be 80%.

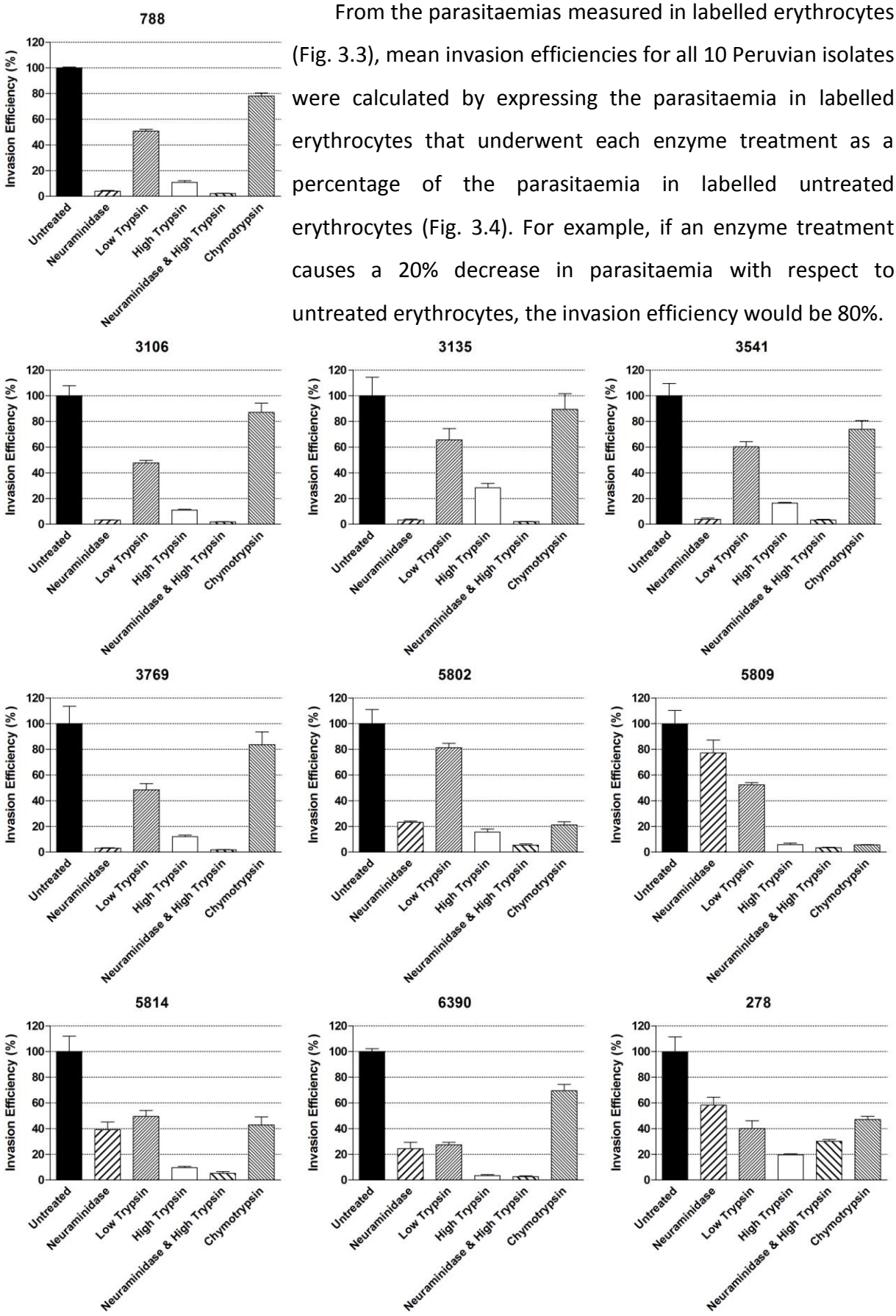

Fig. 3.4. Invasion phenotypes of Peruvian field isolates. Error bars are SEMs.

Clustering of Invasion Phenotypes

Comparison of the invasion profiles of all ten isolates revealed two clusters of phenotypes. This can be seen when invasion profiles are ordered according to their neuraminidase sensitivity (Fig. 3.5). Five isolates exhibited very high sensitivity to neuraminidase and high trypsin but were chymotrypsin-resistant. The isolates of this cluster were 788, 3106, 3135, 3541 and 3769 and are referred to hereafter as Type I phenotypes. The remaining isolates, 278, 5802, 5809, 5814 and 6390, were not grouped by specific criteria but lacked the characteristics of the Type I cluster and were therefore classified as having a Type II phenotype. The differences between the two clusters are summarised in Table 3.2.

	Phenotype Cluster % mean (SEM)	
Enzyme Treatment	**Type I**	**Type II**
Neuraminidase	3.5 (0.2)	44.5 (10.4)
Low Trypsin	54.7 (3.6)	50.3 (8.9)
High Trypsin	15.7 (3.3)	10.8 (3.0)
Neuraminidase & High Trypsin	2.3 (0.3)	9.4 (5.2)
Chymotrypsin	82.5 (2.9)	32.0 (10.5)

Table 3.2. Mean invasion efficiencies for isolates of each phenotype cluster. Standard error of the mean (SEM) is in brackets. All figures are given as percentages (%).

Greater heterogeneity existed in Type II phenotypes than Type I, with no two isolates having identical phenotypes. Within Type II parasites, similarities could be drawn between the invasion profiles of 5802, 5814 and 278, with neuraminidase and chymotrypsin sensitivity appearing to be linked. However, 6390 had high sensitivity to neuraminidase but was relatively chymotrypsin-resistant and of the Type II phenotypes it bore the most resemblance to a Type I profile. Conversely, 5809 had high resistance to neuraminidase treatment but was highly sensitive to chymotrypsin. 278 had unusually high resistance to the combined treatment of neuraminidase and high trypsin, with mean invasion efficiency being 30.2% (SEM 1.4%). The greater variation found amongst Type II phenotypes is evident from the greater SEM values (except for high trypsin treatment: Table 3.2). In general, this cluster showed greater resistance to neuraminidase than Type I isolates with 5802 having the lowest invasion efficiency into neuraminidase-treated erythrocytes (23.2%, SEM 1.0%). As with Type I, high sensitivity to high trypsin treatment was a feature of all Type II phenotypes but, with the exception of 6390, Type II isolates had mean invasion efficiencies under 50% into chymotrypsin-treated erythrocytes. The variation in invasion efficiency between individual isolates is illustrated in Fig. 3.5.

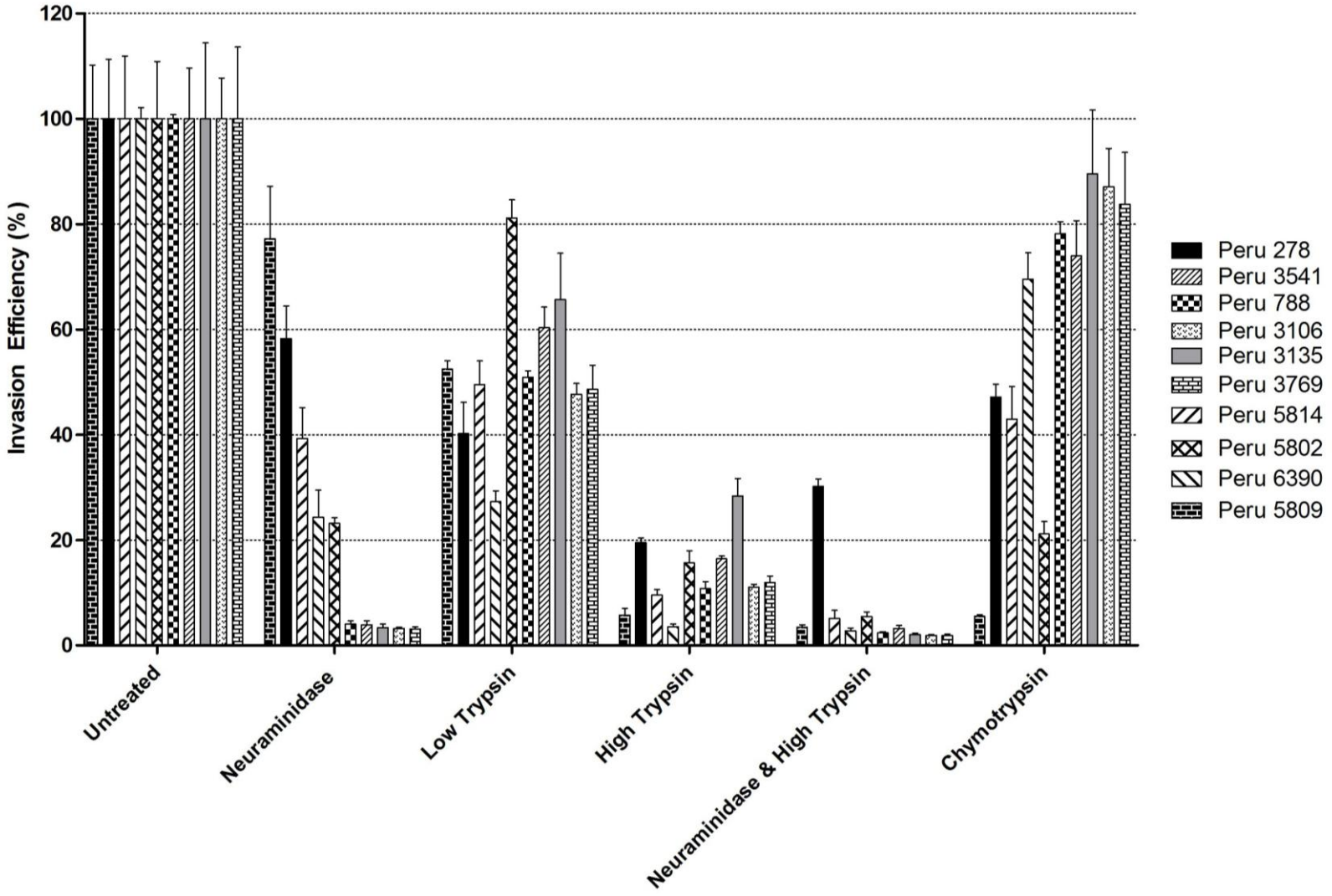

Fig. 3.5. Invasion profiles of all Peruvian isolates. Strains are ordered by decreasing neuraminidase sensitivity, so that the first five isolates for each enzyme treatment correspond to the Type II phenotypes.

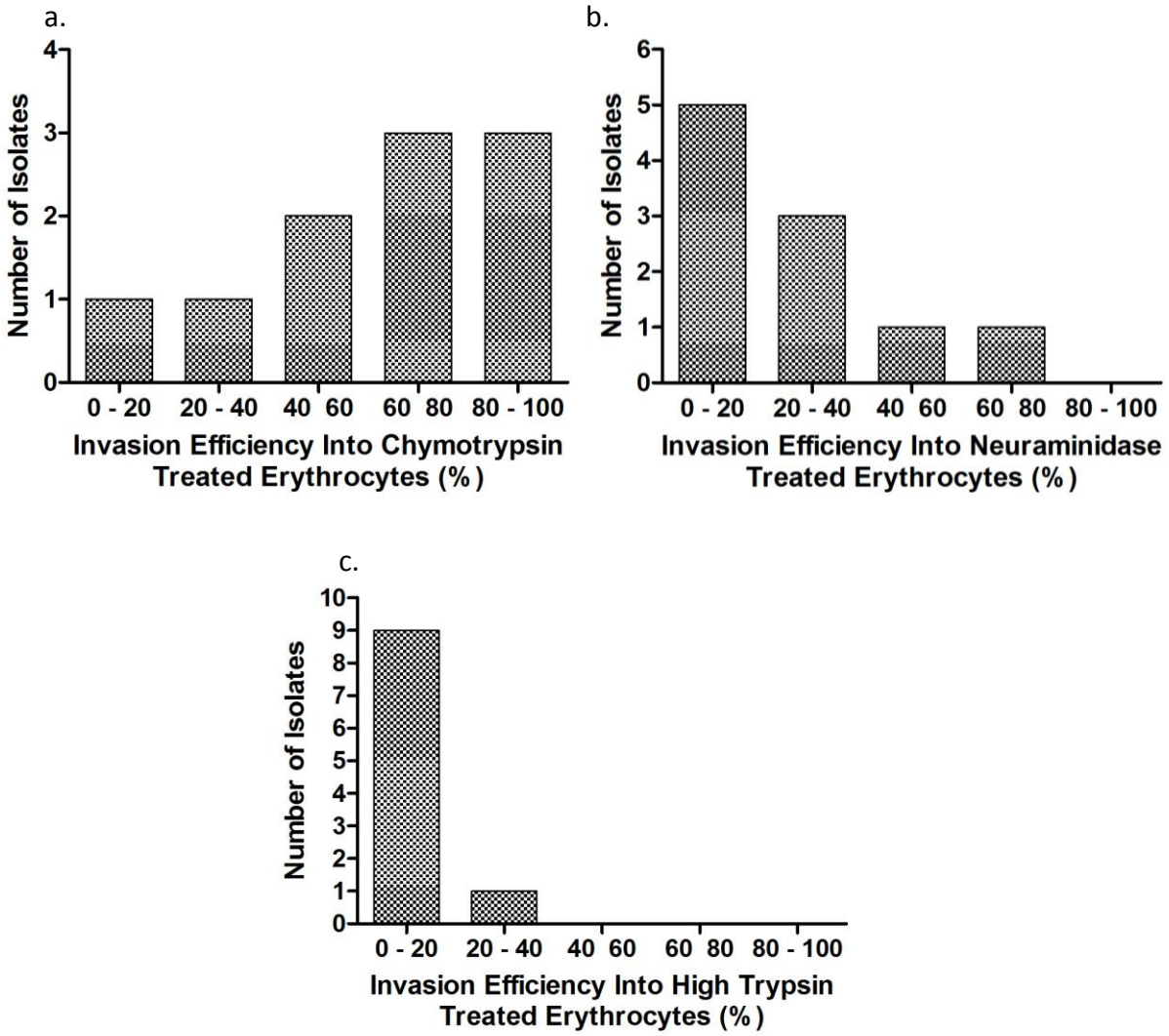

Fig. 3.6. Invasion efficiency into enzyme treated cells. (a) chymotrypsin, (b) neuraminidase, (c) high trypsin.

Across all ten Peruvian isolates invasion efficiency into chymotrypsin-treated cells showed the greatest diversity, ranging from 7.3% (5809) – 89.5% (3135) and also the most even distribution of values (Fig. 3.6a). Inhibition of invasion by neuraminidase treatment resulted in a range of invasion efficiencies from 3.1% (3769) to 70.9% (5809) (Fig. 3.6b). However, despite the large range, the majority of isolates had invasion efficiencies <25% into neuraminidase-treated cells and all isolates with Type I invasion profiles fell into this category. The least variation amongst isolates was seen when invading high trypsin-treated erythrocytes, all but one isolate (3135 – 28.4%) having an invasion efficiency under 20% (Fig. 3.6c).

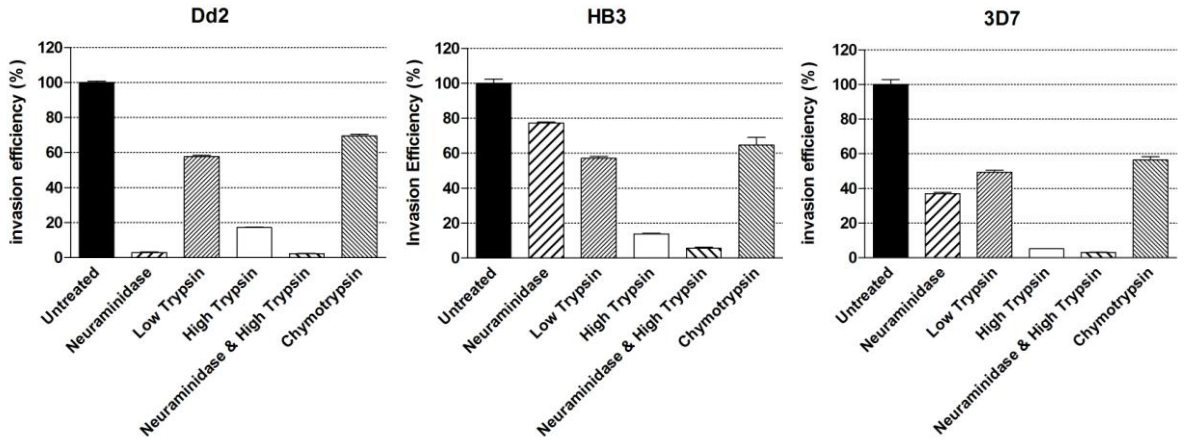

Fig. 3.7. Invasion profiles of lab strains Dd2, HB3 and 3D7. Error bars are SEMs.

Comparing the invasion profiles of Peruvian field isolates to lab strains (Fig. 3.7) illustrates that the Type I phenotypes are very similar to that of Dd2, a strain that originates from South-East Asia. The invasion profiles of Type II isolates are clearly different as they are not completely dependent on neuraminidase-sensitive pathways. 5814 and 5802 are comparable in profile to 3D7 (a lab strain that originates from Africa), while 278 appears more similar to HB3 (a lab strain that originates from Honduras). The invasion efficiency of 6390 into neuraminidase-treated cells is low, falling between the sensitivities of 3D7 and Dd2, while its ability to invade chymotrypsin-sensitive cells is high, similar to Dd2 and HB3. 5809 exhibits neuraminidase sensitivity comparable to HB3, but is unique in its relative inability to invade chymotrypsin-treated cells. This range of phenotypes within Type II isolates emphasises the fact that erythrocyte invasion is a very variable phenotype, even in a region of low malaria transmission and low *P. falciparum* genetic diversity such as the Peruvian Amazon.

Correlations within Invasion Phenotypes and Between Invasion and Multiplication Rates

In addition to invasion profiling, parasite multiplication rates (PMRs) were calculated for each isolate during phenotyping by dividing the final parasitaemia in untreated erythrocytes by the starting parasitaemia of 0.75% (as detailed in Chapter 2: “Materials & Methods”). The final parasitaemia was determined from Hoechst 33342 or SYBR Green I positive events in both donor and target erythrocytes (i.e. the top two populations of the

dot plot in Fig. 3.1), and assumes that all parasites detected in the donor cells are new invasions (Fig. 3.8).

The PMR for Peruvian strains fall into the same clusters produced by invasion profiling. For isolates with Type II invasion profiles, PMR values were uniformly low with a mean of 2.6 (SEM 0.4). Isolates with a Type I invasion phenotype had higher but more variable PMRs with a mean of 10.2 (SEM 1.7). Peruvian isolate 788 had a particularly high PMR of 16.1, and both 788 and 3541 exceeded the PMR of Dd2, the highest of the three lab strains. HB3 had the lowest PMR of a lab strain at 6.8, and the lowest PMR found in a field isolate with a Type I invasion profile was 6.6 in isolate 3106.

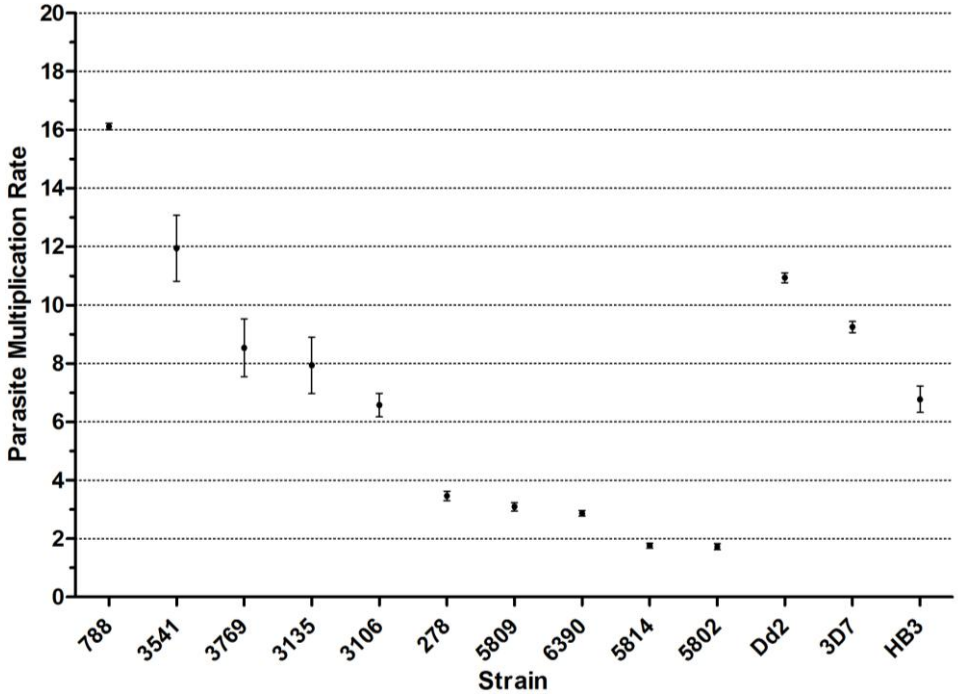

Fig. 3.8. Parasite Multiplication Rates (PMRs) found in Peruvian field strains and three lab strains, Dd2, 3D7 and HB3. PMRs fall into the same clusters as seen in invasion profiles with isolates that have Type I invasion profiles also having PMRs of above 6, while Type II invasion profiles correlate to a PMR below 4.

Invasion efficiencies of the ten isolates were compared for correlation between different enzyme treatments (Fig. 3.9). No correlation was found between invasion into neuraminidase and high trypsin-treated cells (Rs = -0.35, *P* = 0.33; Fig. 3.9c), or invasion into high trypsin-treated and chymotrypsin-treated cells (Rs = 0.37, *P* = 0.30; Fig. 3.9b). However, invasion efficiency into neuraminidase- and chymotrypsin-treated erythrocytes had a strong negative correlation (Rs = -0.85, *P* = 0.0029; Fig. 3.9a).

Given the fact that Type I and II isolates had substantially different mean PMRs and the two clusters differed in their sensitivity to neuraminidase treatment, the PMR for each isolate was also compared to invasion efficiencies into enzyme-treated erythrocytes (Fig. 3.10). Positive correlation was found between PMR and invasion efficiency into chymotrypsin-treated erythrocytes (r_s = 0.73, P = 0.02; Fig. 3.10a). A positive correlation was also found between invasion into neuraminidase-treated erythrocytes and PMR, but it was not statistically significant (r_s = 0.61, P = 0.07; Fig. 3.10b). No correlation was found between invasion into trypsin-treated erythrocytes and PMR (r_s = 0.32, P = 0.37; Fig. 3.10c).

The phenotyping data therefore indicate that the Peruvian isolates fall into two distinct clusters. Type I isolates have variable but generally high PMR and invasion of these isolates is strongly and uniformly inhibited by neuraminidase treatment but is resistant to chymotrypsin treatment. Type II isolates have uniformly low PMR but more variable invasion phenotypes, which are generally characterised by some level of resistance to trypsin treatment. In order to establish whether a genetic basis for these differences could be identified, genomic DNA from all isolates was submitted for whole-genome re-sequencing using an Illumina IIx Genome Analyzer.

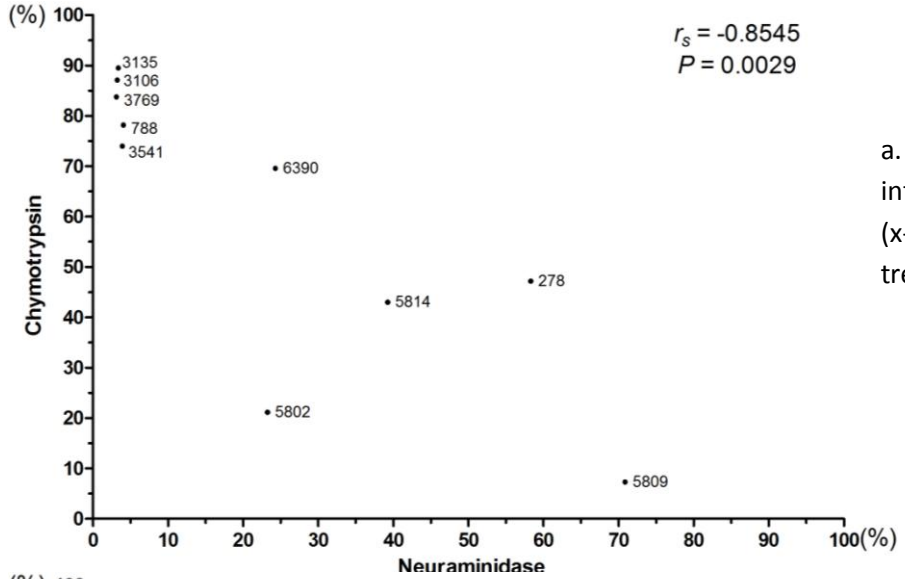

a. Invasion efficiencies (%) into neuraminidase treated (x-axis) and chymotrypsin treated (y-axis) erythrocytes.

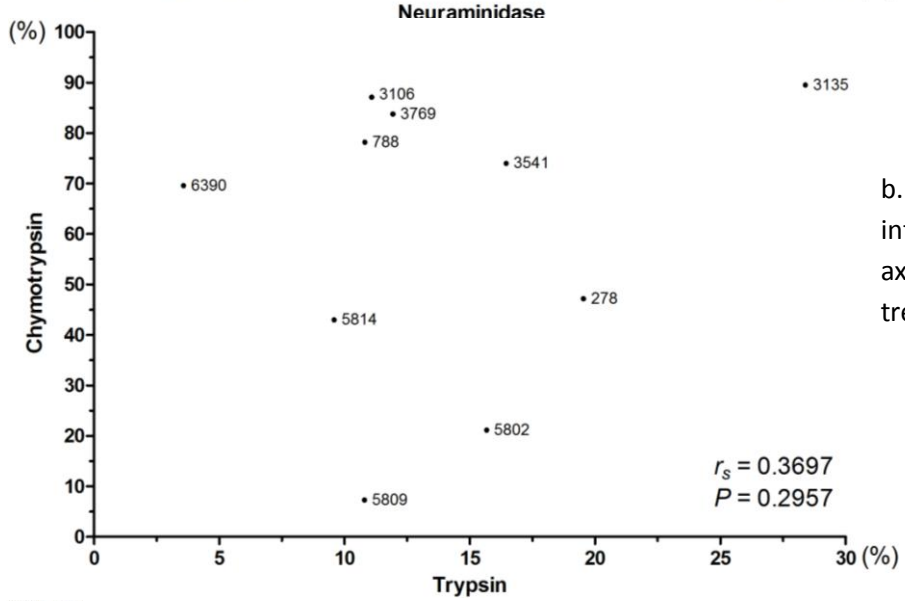

b. Invasion efficiencies (%) into high trypsin treated (x-axis) and chymotrypsin treated (y-axis) erythrocytes.

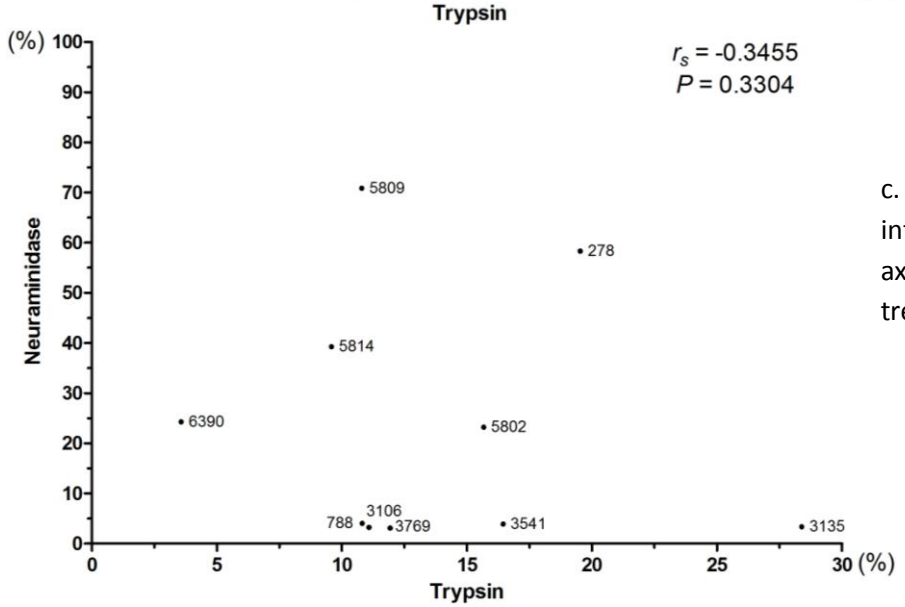

c. Invasion efficiencies (%) into high trypsin treated (x-axis) and neuraminidase treated (y-axis) erythrocytes.

Fig. 3.9. Invasion efficiencies of Peruvian field isolates into enzyme treated erythrocytes. Spearman's rank correlation coefficient (r_s) and a two-tailed *P*-value are given for each plot. Correlation with a *P*-value of <0.05 was considered significant.

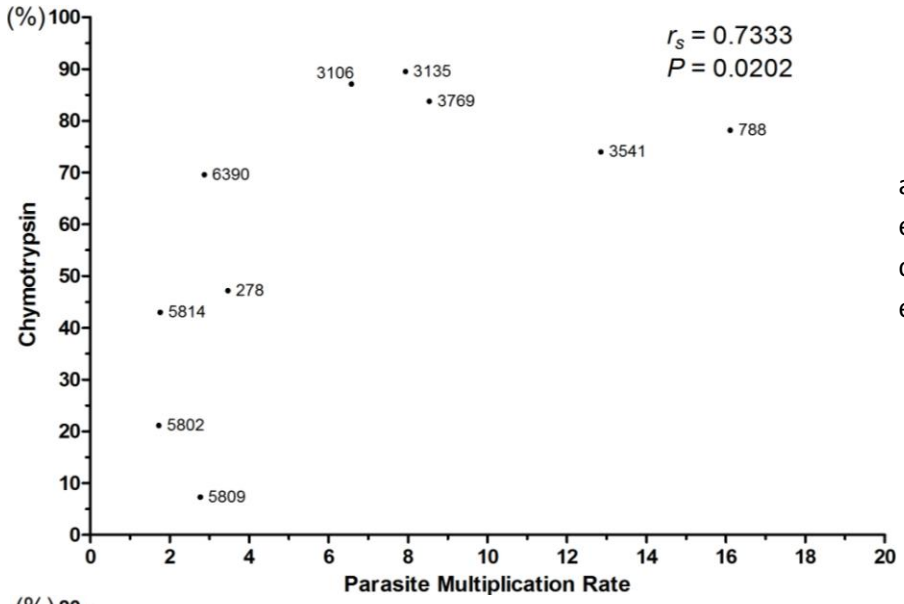

a. PMR (x-axis) and invasion efficiency (%) into chymotrypsin treated erythrocytes (y-axis).

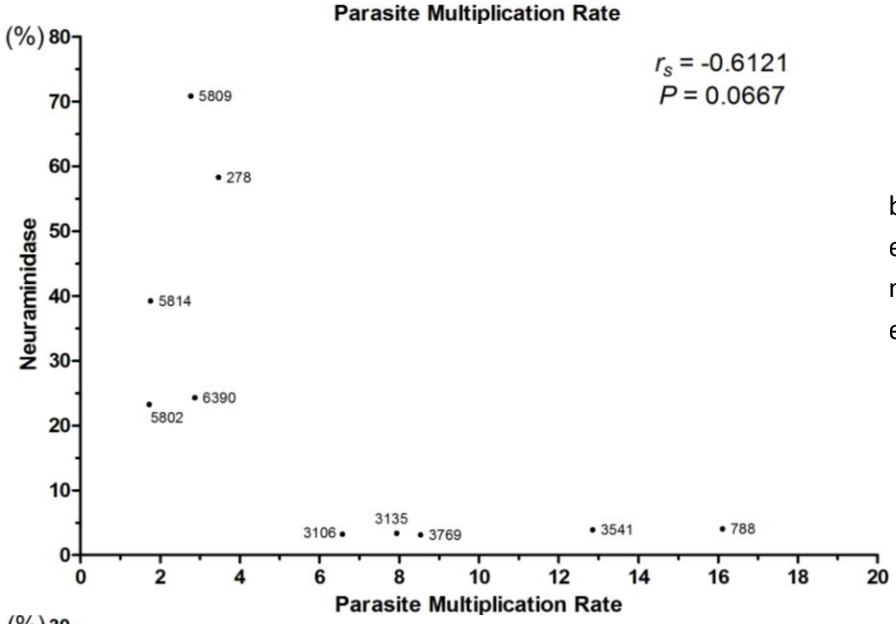

b. PMR (x-axis) and invasion efficiency (%) into neuraminidase treated erythrocytes (y-axis).

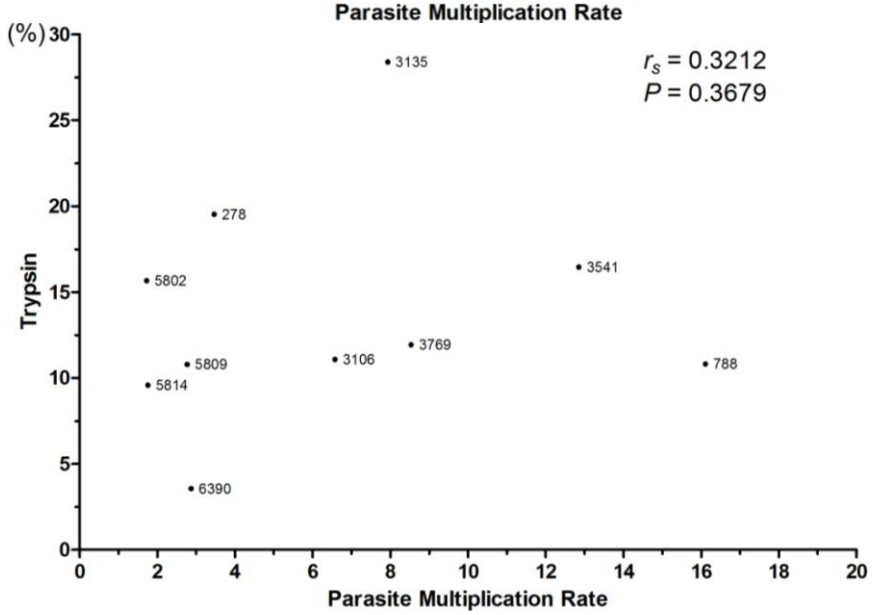

c. PMR (x-axis) and invasion efficiency (%) into high trypsin treated erythrocytes (y-axis).

Fig. 3.10. Invasion efficiencies into enzyme treated erythrocytes and PMR of Peruvian field isolates. Spearman's rank correlation coefficient (r_s) and a two-tailed *P*-value are given for each plot. Correlation with a *P*-value of <0.05 was considered significant.

Genotyping

Analysis of the samples was carried out using MapSeq – a web browser-based tool for comparison of samples (Fig. 3.11), LookSeq – a web browser-based interface for visualising Illumina reads (Fig. 3.12), and Mutabo! – a tool for correlating non-synonymous SNPs to corresponding amino acid changes. All three tools were developed by Dominic Kwiatkowski's team at WTSI.

Fig. 3.11. The MapSeq interface. Genotyping view allows the user to select samples and genome region and identifies the SNPs present with respect to the 3D7 reference sequence. The "compare groups" function creates a list of mutations that are present across a cohort of samples. Analysing populations uses principal component analysis (PCA) to compare different samples.

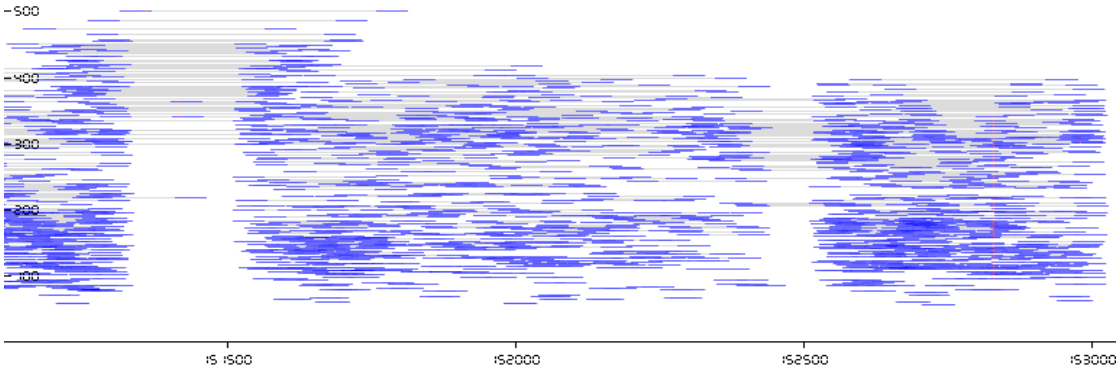

Fig. 3.12. The LookSeq genome browser: a short segment of chromosome 1 of Peruvian isolate 3135. Base number is plotted on the x-axis, and paired read length is on the y-axis. Reads are in blue, the darker blue indicates greater coverage of that area. The grey strips indicate the sequence between paired reads. Red areas signify SNPs called with respect to the 3D7 reference sequence (far right). On the left is an insertion / deletion characterised by the gap in reads and the increase in paired read length either side.

All eleven of the cultured Peruvian field isolates were sequenced using the Illumina platform. Of the eleven isolates, only seven had undergone genome assembly and been analysed at the time of thesis submission, the remaining four are still in the sequencing pipeline. The seven isolates to be analysed include all those with Type I invasion profiles (788, 3106, 3135, 3541 and 3769), one Type II isolate (6390), and one isolate that was not phenotyped because it could not be re-cultured after freezing (9050). 278, 5802, 5809 and 5814 are still in the sequencing pipeline.

Principal component analysis (PCA) was used to compare SNPs in Peruvian isolates to previously sequenced samples from other isolates (Fig. 3.13). PCA is useful for identifying patterns in data and displaying the results to highlight their similarities and differences, and is particularly useful when there is a large number of variables. By transforming data values to new sets of variables, the principal components, the dimensionality of the data set is reduced but the majority of the variability is retained (Jolliffe 2002). The majority of variability is summarised in the principal component (x-axis), while remaining variability is assessed in the second principal component (y-axis). In the context of *Plasmodium* genotyping, samples can be analysed using two principal components. Isolates will group together if they are genetically similar and will be separated if they are genetically diverse. This allows a large number of samples to be compared for similarities quickly and simply.

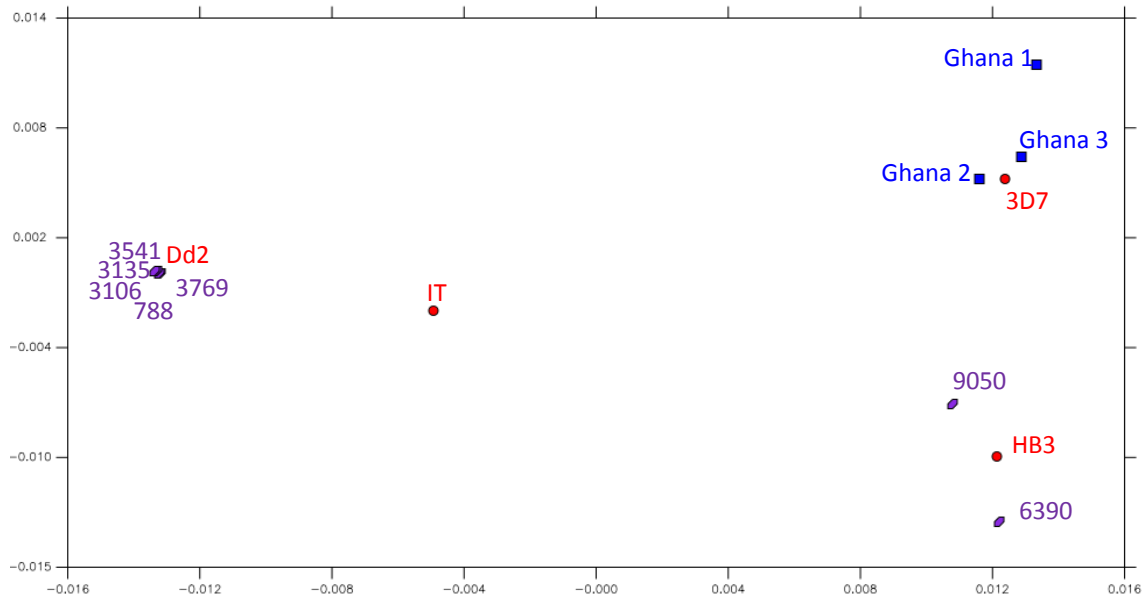

Fig. 3.13. PCA plot of all sequenced *Plasmodium* samples. Peru strains are purple hexagons, red circles are lab strains and blue squares are field isolates from Ghana. The plot is generated from PCA analysis of all SNPs found in the genome, with the minimum of ten reads for a SNP call to be made.

The PCA plot (Fig. 3.13) shows that two of the Peruvian isolates are genetically similar to the lab strain HB3 originally from Honduras. The remaining five Peruvian isolates that all had Type I invasion profiles are genetically very similar to Dd2 (Fig. 3.13 / Fig. 3.14). The field isolates from Ghana group with 3D7, a lab strain thought to originate from Africa. IT, another lab strain originating from Brazil, does not appear to be genetically similar to the other isolates studied here.

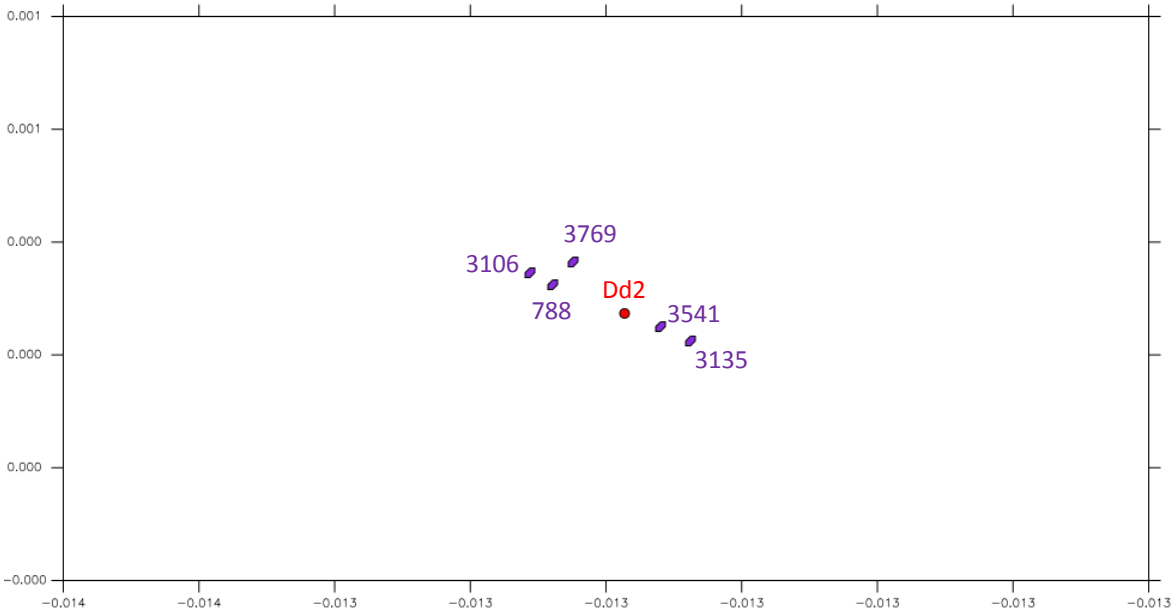

Fig. 3.14. Peruvian isolates with type one invasion profiles are closely related to Dd2. This is a magnified view of the group on the extreme left of Fig. 3.13. As can be seen from the scales, there is virtually no variation between these isolates. Peruvian isolates are represented as purple hexagons, while Dd2 is a red circle.

The genomic similarities between Peruvian isolates with Type I phenotypes and Dd2 were consistent with the similarities seen in phenotype. However, two features of the PCA plot were unusual. Firstly, the genetic distance between the Type I isolates and Dd2 was significantly lower than the distance between any two of the 400 *P. falciparum* isolates that have now been sequenced at WTSI (Kwiatkowski et al. unpublished data). Secondly, at the scale of PCA shown in Fig. 3.13, *P. falciparum* isolates always group by geographic origin. The fact that Type I Peruvian isolates cluster with a South Asian strain, while two other Peruvian isolates cluster with a strain from Honduras is unusual. The simplest explanation of the data is that the Type I Peruvian isolates were contaminated with a Dd2 like strain.

To test this hypothesis, all isolates that had Type I invasion profiles were tested for *msp*-1 and *msp*-2 genotypes. MSP-1 and MSP-2 are encoded by highly variable genes (*msp1* and *msp2* respectively) that are routinely used for genotyping studies (Baum et al. 2003; Lobo et al. 2004; Deans et al. 2007). The *msp1* block 2 and *msp2* block 3 loci containing highly polymorphic repeat sequences were amplified by PCR and the sizes of DNA fragments produced were analysed by gel electrophoresis (Table 3.3).

	Fragment size (bp)	
Isolate	***msp1***	***msp2***
3D7	472	748
Dd2	430	515
W2	436	513
3135	431	513
3541	435	510
788	430	518
3769	436	514
3106	434	514
9050	455	854
6390	469	790
278	467	776
5802	428	680
5809	454	848

Table 3.3. Fragment sizes of polymorphic loci from *msp1* and *msp*2. Highlighted in red are fragment sizes from Peruvian isolates that had loci that were of very similar size to lab isolates Dd2 or W2.

All Type I isolates that were found to be genetically similar to Dd2 by PCA had polymorphic fragment sizes from *msp1* block 2 and *msp2* block 3 that were homologous to Dd2 (highlighted in red in Table 3.3). In contrast, Type II isolates had clearly different *msp1* and *msp2* genotypes; although the fragment of *msp1* amplified from Peruvian isolate 5802 was similar to Dd2 the *msp2* fragment was very different.

From the identical phenotypes, PCA and polymorphic fragment sizes it was clear that Peruvian isolates 3135, 3541, 788, 3769 and 3106 were contaminated. While Dd2 had never been grown in Peru, its parental lab strain W2 had been in culture in Iquitos on multiple occasions as a positive control for the culture procedure. Checking the culture records at UNAP established that W2 was in culture at the times when the Type I isolates had been

frozen. Conversely, when the non-contaminated isolates (278, 5802, 5809, 5814 and 6390) had been in culture, W2 was not being grown.

Non-Synonymous SNPs and Amino Acid Changes in Peruvian Isolate 6390

Of the non-contaminated samples only 6390 had been genotyped at the time of thesis submission; sequences for the remaining isolates are expected within the next month. For this isolate, non-synonymous SNPs were identified across 62 genes identified as having a role in invasion, and the consequent amino acid changes were determined. The data are summarised below and are presented in full in Appendix Table A2.

98 non-synonymous SNPs were identified in these 62 genes. The mean number of reads for non-synonymous SNP calls was 86, but five SNPs were called from fewer than ten reads resulting in a lower confidence in the calls. The 93 high confidence non-synonymous SNPs code for 80 amino acid changes, the disparity between numbers of SNPs and amino acid changes being due to multiple SNPs being present in a single codon.

Of the genes known to act as invasion ligands, no SNPs were found in PfRh2a, PfRh2b, PfRh4, EBL-1 or EBA-181. However, a single SNP was found in each of EBA-140, EBA-175 and PfRh5. The greatest level of polymorphism that was observed in an invasion ligand was in PfRh1, with eight SNPs. MSP3.8, a protein of unknown function that is a member of the MSP3 gene family on chromosome 10 (Singh et al. 2009), had the largest number of SNPs (45), suggesting that it is highly polymorphic between isolates.

With more sequences available, correlation between ligand sequence and invasion phenotype will be possible, as discussed below.

RNA Extraction

RNA was extracted from all isolates that were phenotyped. The minimum quantity extracted from an isolate was 1.87 µg from 3106 (Appendix Table A1). As 10 µg is the current lower limit for RNASeq, transcriptomic analysis of these isolates awaits further technology improvement.

Extra Populations

Invasion phenotyping of two Peruvian isolates yielded an additional cell population not visible in any of the other samples. The invasion assays using the two-dye method routinely yielded four clearly separable populations observed by flow cytometry without using a post-invasion trypsin treatment (Figs. 3.1 & 3.15 a). However, in the case of Peruvian strains 3135 and 3769 extra populations with an intermediate level of DNA staining were observed (Fig. 3.15 b & c), which made parasite quantification difficult.

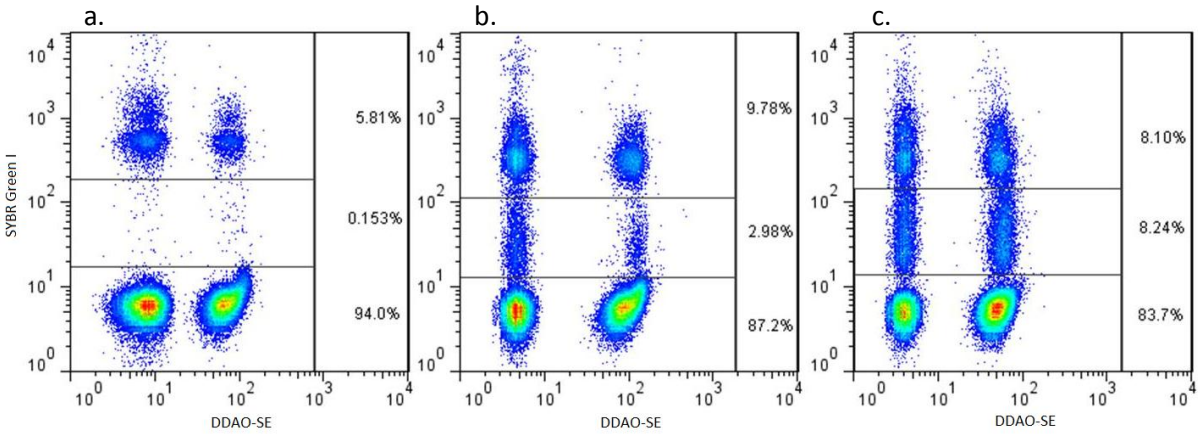

Fig. 3.15. Dot plots from Peruvian phenotyping assays of the invasion of erythrocytes that have not been enzyme treated. Staining: DDAO-SE (x-axis), SYBR Green I (y-axis). (a) 788; (b) 3135; (c) 3769. 788 produced four well separated populations as expected, also seen in Fig. 3.1. 3135 and 3769 have an extra, intermediate population between events that are SYBR Green I positive (parasitised) and SYBR Green I negative (uninfected).

For all strains previously studied, gates could be manually placed to count the events in each quadrant. With the four populations of 3135 and 3769 having a “smear” between them, accurate manual gating was impossible due to the diffuse boundary between events caused by uninfected erythrocytes and parasitised events. The extra populations were also highly consistent and always present in invasion assays using these two isolates, regardless of whether SYBR Green I or Hoechst 33342 was used to stain DNA.

This section deals with the two questions that were asked of the extra populations observed by flow cytometry: How can strains showing this phenomenon be accurately phenotyped, and what are the causes of this population?

Quantification of the Intermediate Population

Quantification of the intermediate population was compared across all Peruvian isolates by manually placing gates around each intermediate population (as shown in Fig. 3.15) for positive control invasion wells, where invasion is carried out using labelled untreated erythrocytes. The results are displayed in Fig. 3.16; points are the mean of three replicates, and error bars represent SEM.

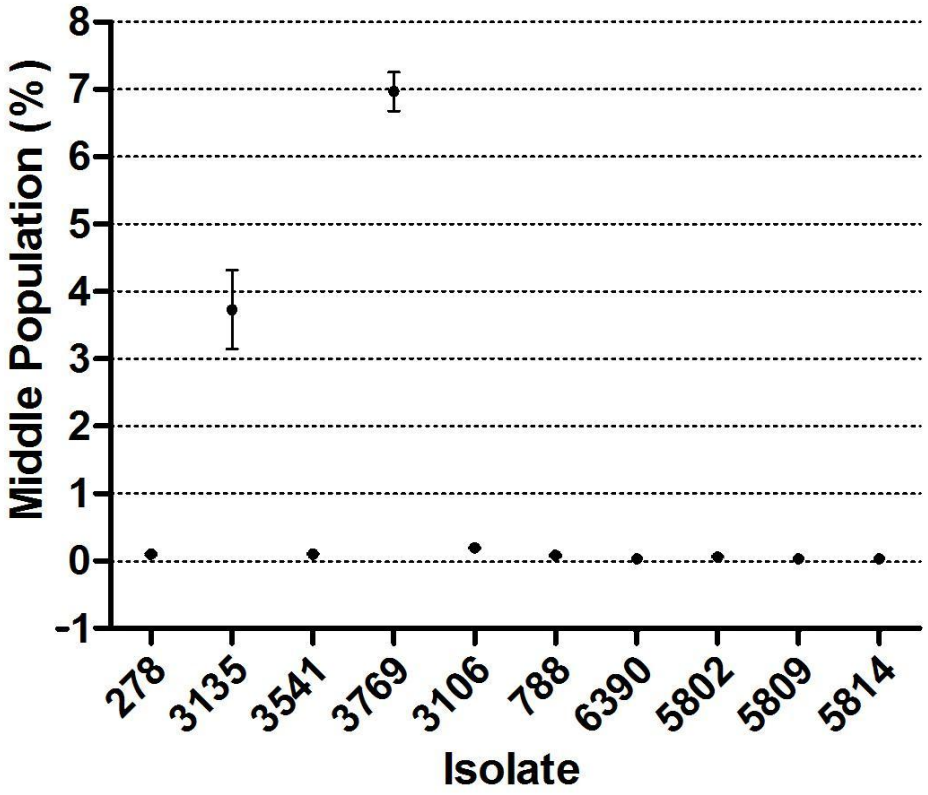

Fig. 3.16. Quantification of the intermediate population in Peruvian field isolates. By using manual gating the intermediate population is represented as a percentage of all events observed by flow cytometry.

Fig. 3.16 shows that only in two Peruvian isolates, 3135 & 3769, is the intermediate population of significant size. In 3135 the mean size of the intermediate population is 3.73% (SEM 0.59) of the sample; in 3769 it is 6.97% (SEM 0.29). In the other samples the intermediate population is negligible; 3106 is the largest of these, representing 0.20% (SEM 0.009) of the sample. In all samples other than 3135 and 3769 when the intermediate population is small the exact placement of the gate has an insignificant effect on the overall parasitaemia recorded (Fig. 3.15 a). However, for isolates 3135 and 3769 a small difference in gate placement could have a large effect on the recorded parasitaemia (Fig. 3.15 b & c).

The Intermediate Population: Parasite-based Events?

To determine whether the intermediate population is comprised of parasitised erythrocytes, an invasion assay was set up with two wells using unstained, untreated erythrocytes mixed with Peruvian isolate 3135. The method was the same as detailed in the "Phenotyping Invasion Assay" section of the "Methods", except the target erythrocytes were not stained and only invasion into erythrocytes that had not been enzyme-treated was studied.

After the 48 hour incubation period, one well was used to make a blood smear on a slide. This slide then underwent methanol fixation and Field's staining, using the standard protocol. The parasitaemia was determined by counting 1,000 erythrocytes and calculating the proportion of infected erythrocytes present by light microscopy.

The other well underwent fixation with 2% PFA / 0.2% GA and Hoechst 33342 staining using the standard protocol. An aliquot of the suspension was placed on a glass slide, air dried and fixed with methanol. The parasitaemia was determined by counting 1,000 erythrocytes and determining the proportion of Hoechst 33342 positive erythrocytes present by fluorescence microscopy. The parasitaemia was also determined by counting 100,000 events from the well using a BD LSRII flow cytometer. The gate placement for determination of parasitaemia by flow cytometry is shown in Fig. 3.17.

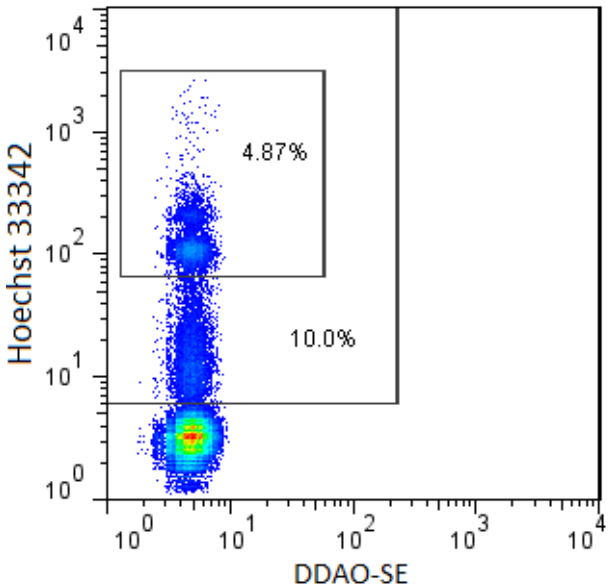

Fig. 3.17. Two different gate placements to determine parasitaemia in Peruvian isolate 3135. One gate was placed around both the intermediate population and the top population (parasitaemia 10.0%). The other gate was placed around only the top population (parasitaemia 4.87%).

Parasite staining	Viewing technique	Parasitaemia (%)
Field's staining	Light microscopy	4.48
Hoechst 33342	Fluorescence microscopy	5.43
Hoechst 33342	Flow cytometry (top population only)	4.87
Hoechst 33342	Flow cytometry (intermediate and top populations)	10.00

Table 3.4. The parasitaemia of Peruvian isolate 3135 determined using different methods.

The parasitaemia determined from the different methods is detailed in Table 3.4. Comparison of parasite counts using the three methods suggest that only the top gate contains events caused by intra-erythrocytic parasites. The parasitaemias determined by Field's staining, fluorescence microscopy and flow cytometry fell within 0.95% of each other when only the top population was defined as parasitic. In contrast, when the intermediate population was also included in the parasitaemia count by flow cytometry, the parasitaemia was 10.00%, significantly different to the microscopy-based counts. Further investigations of the intermediate population are discussed below.

Phenotyping Using Post-Invasion Enzymatic Treatments

As previously discussed, when parasites from isolates 3135 and 3769 invaded erythrocytes that had undergone no enzyme treatment, an extra population was present in both target and donor erythrocytes (Fig. 3.15 b & c). However, the intermediate population was not consistent across the phenotyping invasion assay (Fig. 3.18).

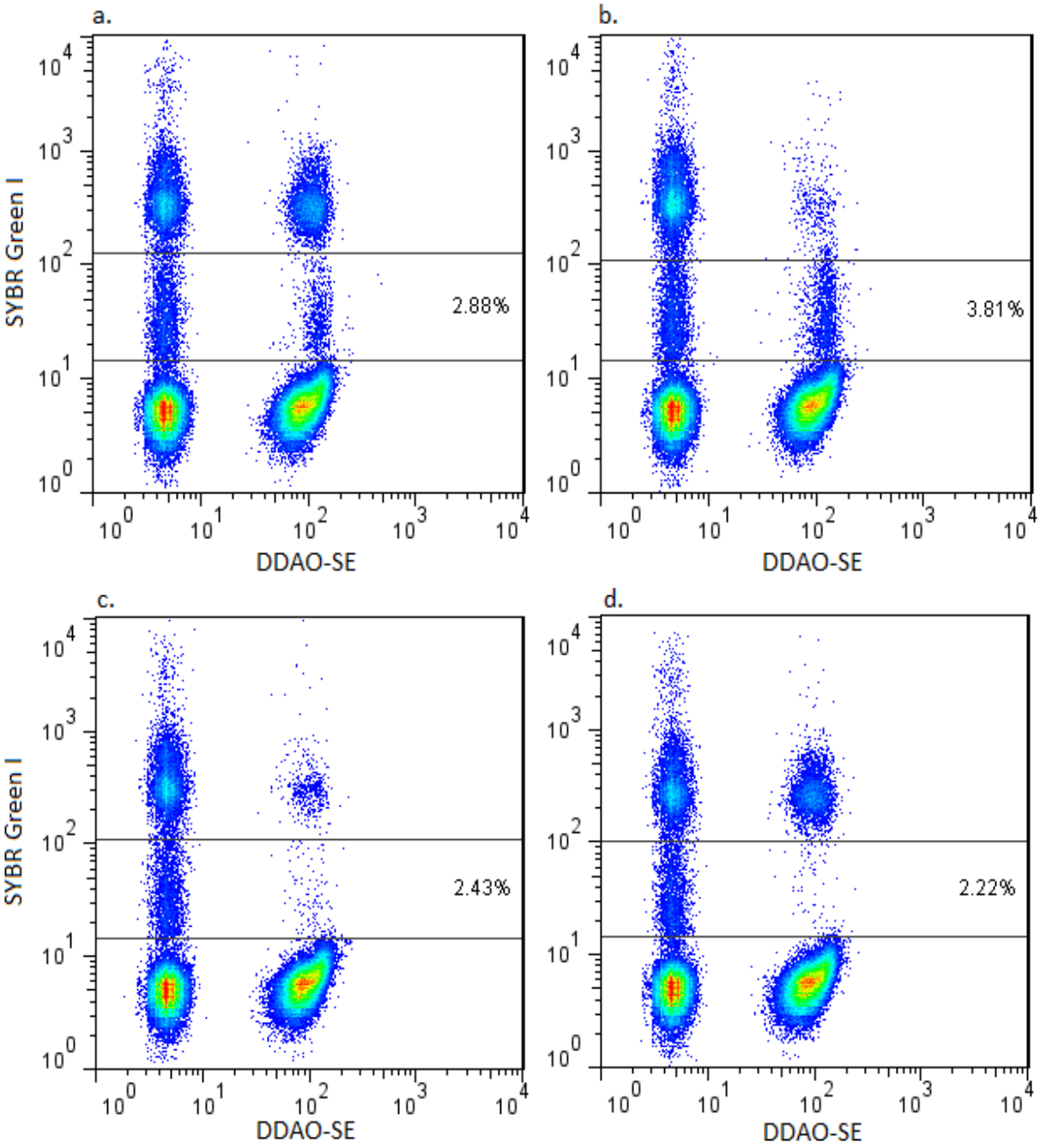

Fig. 3.18. Four flow cytometry dot plots of Peruvian isolate 3135. The target erythrocytes underwent different enzyme treatments: (a) no enzyme treatment; (b) neuraminidase treatment; (c) high trypsin treatment; (d) chymotrypsin treatment.

When the DDAO-SE-labelled, target erythrocytes were treated with trypsin or chymotrypsin the population was greatly reduced in labelled erythrocytes, but not in unlabelled erythrocytes (Fig. 3.18 c & d). However, neuraminidase treatment of target erythrocytes had no effect on the intermediate population (Fig. 3.18 b). This observation suggests that trypsin or chymotrypsin treatment of erythrocytes could eliminate the intermediate population.

To test this hypothesis an invasion assay was set up using unlabelled, untreated cells in the standard manner but, after 48 hours of *in vitro* culture, the cell pellet underwent one of four different treatments:

- Treatment A: Control. Cells resuspended in 100 µL PBS.
- Treatment B: 100 µL 20mU/mL neuraminidase was added to each well and the suspension mixed thoroughly.
- Treatment C: 100 µL 1 mg/mL trypsin was added to each well and the suspension mixed thoroughly.
- Treatment D: 100 µL 1 mg/mL chymotrypsin was added to each well and the suspension mixed thoroughly.

After individual treatments the plate was incubated for one hour at 37°C before all wells were washed with PBS and stained with Hoechst 33342 using the previously described method. Wells were acquired using a BD LSRII flow cytometer and 100,000 events were counted.

The effects of the post-invasion enzymatic treatments are shown in Fig. 3.19. Neuraminidase treatment (Fig. 3.19 b) had no impact on the intermediate population. However both trypsin and chymotrypsin removed the intermediate population while having no impact on the top population (Hoechst 33342 positive), believed to be the true parasitaemia.

Although chymotrypsin appeared just as effective as trypsin at removing the extra populations, trypsin was used for further experiments.

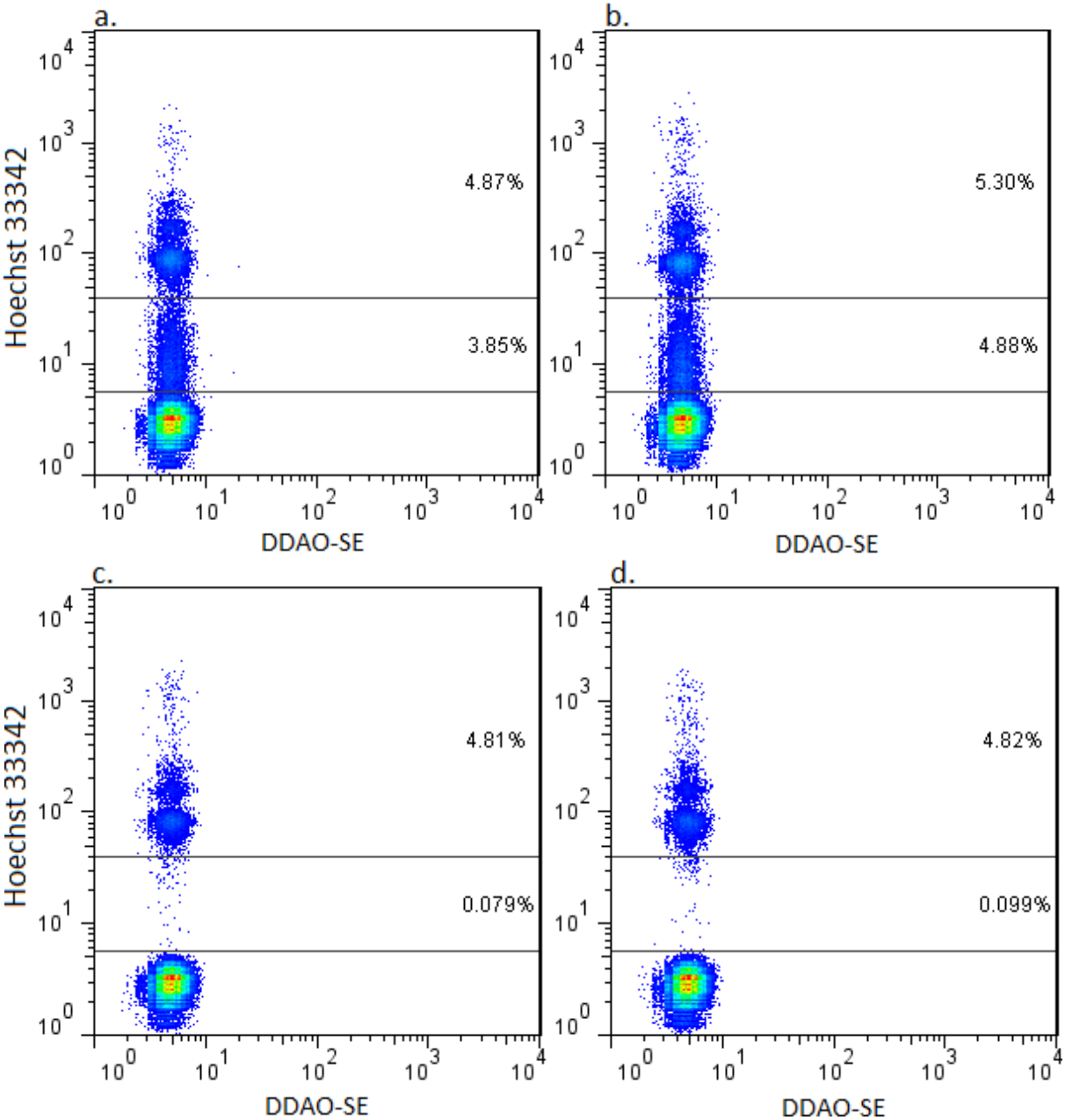

Fig. 3.19. The effects of post-invasion enzymatic treatments on the intermediate population.
(a) No enzyme treatment; (b) neuraminidase treatment; (c) trypsin treatment; (d) chymotrypsin treatment.

Validation of Post-Invasion Trypsin Treatment

Confirmation was required that the post-invasion trypsin treatment did not have a significant impact upon parasitaemia and could therefore be used in phenotyping invasion assays. 3D7 and Dd2, two lab strains that did not have any unexpected extra populations when phenotyped, were used for this purpose.

Invasion assays of 3D7 and Dd2 were set up and carried out exactly as detailed in Chapter 2 “Materials and Methods: Phenotyping Invasion Assay”, with one set of triplicate wells being trypsin-treated after the 48 hour incubation period, and the other set of triplicate wells not undergoing post-invasion treatment. After acquiring the data, the parasitaemia of the two sets of triplicate wells were compared. The experiment was repeated and the combined results of both experiments are shown in Figs. 3.20 & 3.21.

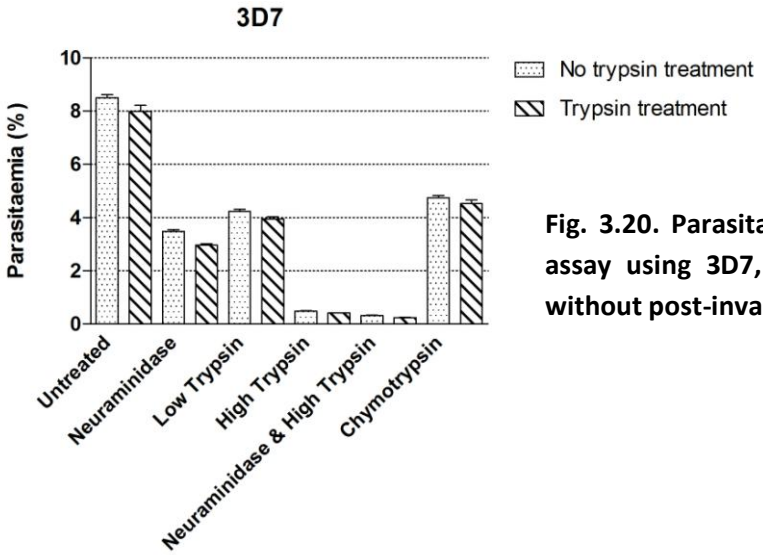

Fig. 3.20. Parasitaemia of a phenotyping invasion assay using 3D7, comparing replicates with and without post-invasion trypsin treatment.

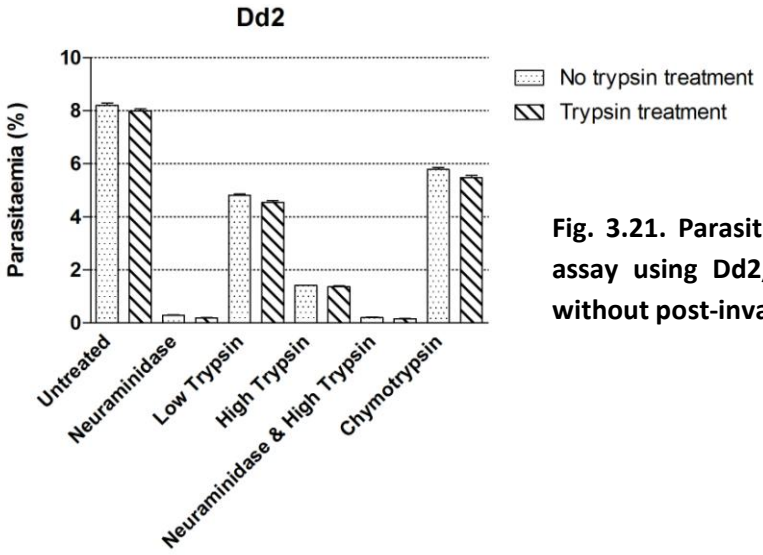

Fig. 3.21. Parasitaemia of a phenotyping invasion assay using Dd2, comparing replicates with and without post-invasion trypsin treatment.

Parasitaemia values for replicates undergoing post-invasion trypsin treatment were very similar to replicates that were untreated post-invasion. There was a slight decrease in mean parasitaemia in all wells where post-invasion trypsin treatment was carried out, ranging from 0.52 ± 0.10 (3D7 – neuraminidase) to 0.04 ± 0.02 (Dd2 – high trypsin and neuraminidase), perhaps due to lysis of protease-treated infected cells.

The confirmation that post-invasion trypsin treatment did not significantly affect the true parasitaemia meant that the two isolates that exhibited the extra population could now be accurately phenotyped. Resolution of this issue meant that all subsequent phenotyping assays were carried out as described in Chapter 2 "Materials and Methods: Phenotyping Invasion Assay", including post-invasion trypsin treatment and Hoechst 33342 staining. Isolates that had been phenotyped prior to this discovery were re-phenotyped using the new method. As discussed previously, phenotypes without post-invasion trypsin treatment do not differ significantly from those that include post-invasion trypsin treatment (Appendix Figs. A1 & A2). The only isolate that was not re-phenotyped using this method was 278, which could not be re-cultured after being frozen. Consequently, the values for 278 calculated in Figs. 3.3 & 3.4 are from an invasion assay using SYBR Green I staining, without post-invasion trypsin treatment.

Determining the Source of the Intermediate Population

Although isolates that displayed an intermediate population, only visualised by flow cytometry, could now be phenotyped for invasion accurately by using a post-invasion trypsin treatment to remove the population, the source of this population was still undetermined. The following experiments were undertaken to verify a number of postulates regarding the cause of the intermediate population.

Erythrocyte Rosetting

Clumping of erythrocytes, or rosetting, is a possible reason for a decrease in fluorescent intensity of DNA stains. It was hypothesised that if one parasitised erythrocyte was surrounded by two or more uninfected erythrocytes, the fluorescence intensity from the stained parasite DNA may essentially be masked by the presence of the surrounding, uninfected cells. The clumping of erythrocytes would be consistent with the post-invasion

protease treatment removing the intermediate population, if the ligands responsible for clumping were being digested by the enzyme.

As well as measuring fluorescence intensity, flow cytometry also measures forward scatter and side scatter from each cell. Forward scatter represents the size of the particle, while side scatter corresponds to the intracellular complexity of the cell. If the intermediate population arose from cell clumps, both forward scatter and side scatter would be expected to differ from that of an individual cell. In Fig. 3.22 forward and side scatter were assessed for Peruvian isolate 3135. Fig. 3.22 b shows the forward and side scatter values for just the intermediate population, a subset of the whole sample of 3135 shown in Fig. 3.22 a. The intermediate population does not appear to have a different size or intracellular complexity compared to the rest of the sample.

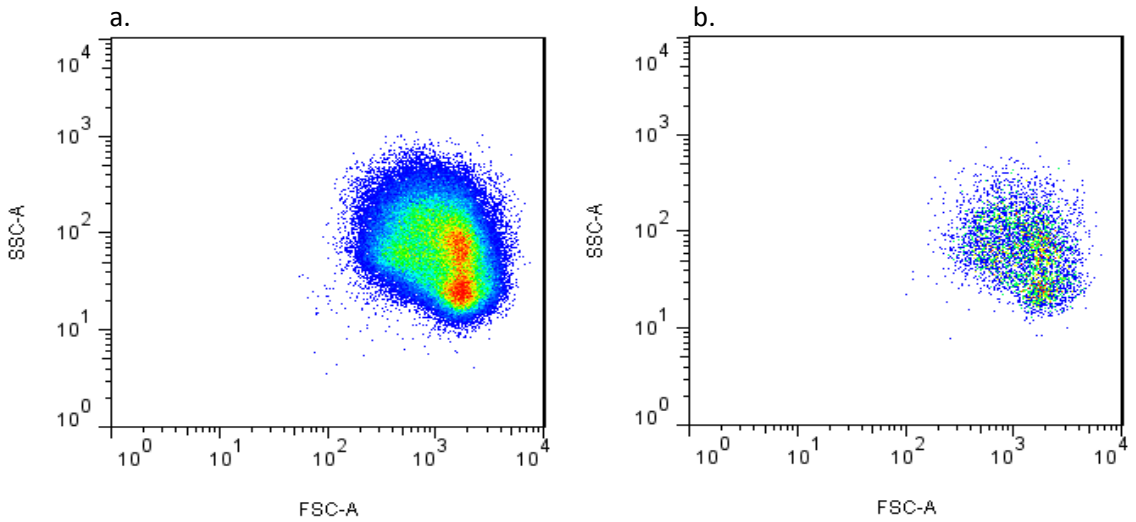

Fig. 3.22. Flow cytometry dot plots of forward scatter (x-axis) and side scatter (y-axis) from Peruvian isolate 3135, to compare the relative size and intracellular complexity of the intermediate population compared to the remainder of the sample. (a) The whole sample of 3135. (b) The intermediate population as a subset of the whole population in (a).

In addition to the flow cytometric analysis of clumping in Fig. 3.22, an erythrocyte rosetting assay was performed using strain 3135 (Chapter 2 "Materials and Methods: Erythrocyte Rosetting Assay"). Using the definition of rosettes as one parasitised erythrocyte in close contact with two or more uninfected erythrocytes, 7/200 parasitised erythrocytes were found in rosettes; a rosetting frequency of 3.5%. In Fig. 3.19 a, the intermediate population is quantified as 3.85% and the parasitised population is 4.87% of the total sample. If every event in the intermediate population involved a rosetted,

parasitised erythrocyte, a rosetting frequency of 44% would be expected. This, combined with the scatter data, suggest that rosettes are not an explanation for the intermediate population.

Merozoite Adhesion

The second possibility was that the intermediate population arose from merozoites adhering to but failing to invade erythrocytes. While a merozoite contains a single copy of the genome and would be expected to bind fluorescent dyes to the same extent as rings or early trophozoites, it cannot survive outside the erythrocyte, and subsequent degradation of the merozoite should lead to a decrease in fluorescence signal.

Variation of the Intermediate Population over the Life Cycle

If merozoite adherence and degradation caused the intermediate population it would therefore be expected that the intermediate population would be at its largest immediately after re-invasion, when the most merozoites are still adhered. This population should then decrease over time. To test this hypothesis, the presence of the intermediate population was measured over time over two separate life cycles of Peruvian isolate 3769. Time course experiments one and two were performed in the same life cycle, while the third experiment was performed in the subsequent life cycle. Time points in the parasite intra-erythrocytic life cycle were estimated by Field's staining and thin smear light microscopy.

Time Course 1 & 2 (h)	Parasite stage
9	Rings
25	Late rings
35	Trophozoites
1	Early rings / late schizonts

Time Course 3 (h)	Parasite stage
43	Late trophozoites / early schizonts
47	Schizonts
3	Early rings / late schizonts
19	Rings
25	Late rings
43	Late trophozoites / early schizonts

Table 3.5. The elapsed time (hours) of the parasite intra-erythrocytic life cycle when measurements of the intermediate population were taken after initiating an invasion assay. It should be noted that the time of the life cycle is an estimate accurate ± six hours. Where more than one parasite life cycle stage was seen in the culture, the predominating stage is listed first.

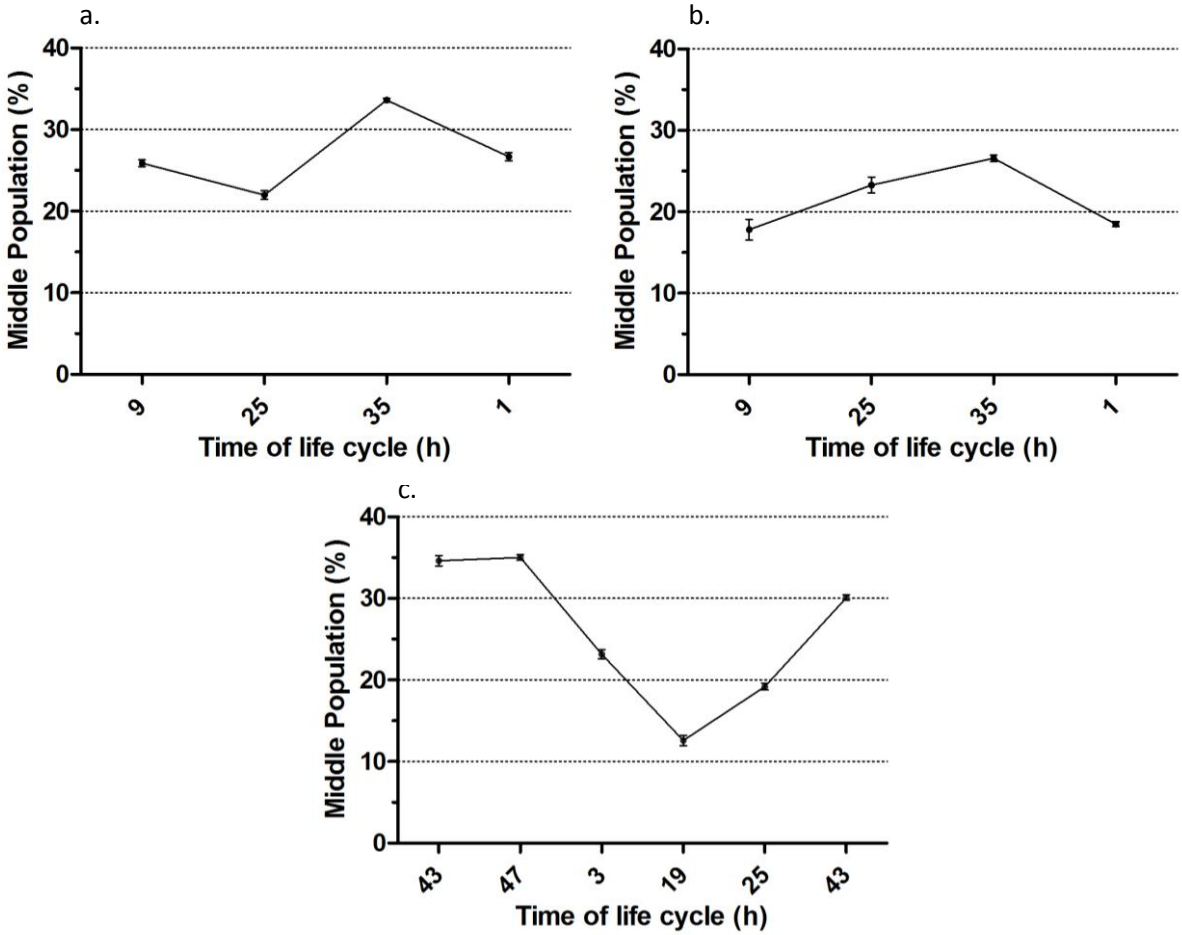

Fig. 3.23. Variation of the intermediate population with life cycle. (a) Time course 1; (b) Time course 2; (c) Time course 3. The intermediate population (y-axis) is expressed as a percentage of the Hoechst 33342 events (the top two populations in Fig. 3.17).

From Fig. 3.23, rather than the hypothesised increase in expression of the intermediate population in the early stages of the parasite life cycle, the population decreased in the ring stage and was largest in the late trophozoite and schizont stages. From the third time course (Fig. 3.23 c), this population accounted for 12.6% (SEM 0.6) of the Hoechst 33342 positive events after 19 ± 6 hours (Hoechst 33342 positive events are the top two populations in Fig. 3.17. This excludes uninfected erythrocytes, which were defined as Hoechst 33342 negative and comprises the bottom population in Fig. 3.17). In the third experiment the population was maximal after 47 hours of the parasite life cycle, representing 35.0% (SEM 0.3) of the Hoechst 33342 positive events. In the first two experiments (Fig. 3.23 a & b), although fewer measurements were taken, the same pattern was apparent with the proportion of Hoechst 33342 positive events present in the intermediate population increasing in later stages of the life cycle.

Anti-MSP-1 19 kDa Antibody Test

To detect specifically the presence of adhered merozoites on the surface of erythrocytes, antibodies to the 19 kDa fragment of MSP-1 were used (Figs. 3.24 to 3.27). MSP-1 is a merozoite surface protein, so would be detectable on extracellular merozoites but not in parasites that have invaded erythrocytes, unless the cells are permeabilised. Peruvian isolate 3769 was used to study the intermediate population, while Peruvian isolate 3541 (which does not express the intermediate population) was used as a control. Anti-MSP-1 19 kDa binding was measured in schizonts and rings using a FITC-conjugated secondary antibody. Anti-MSP-1 19 kDa binding was compared between rings and schizonts, with and without permeabilisation, to differentiate extracellular and intracellular merozoites.

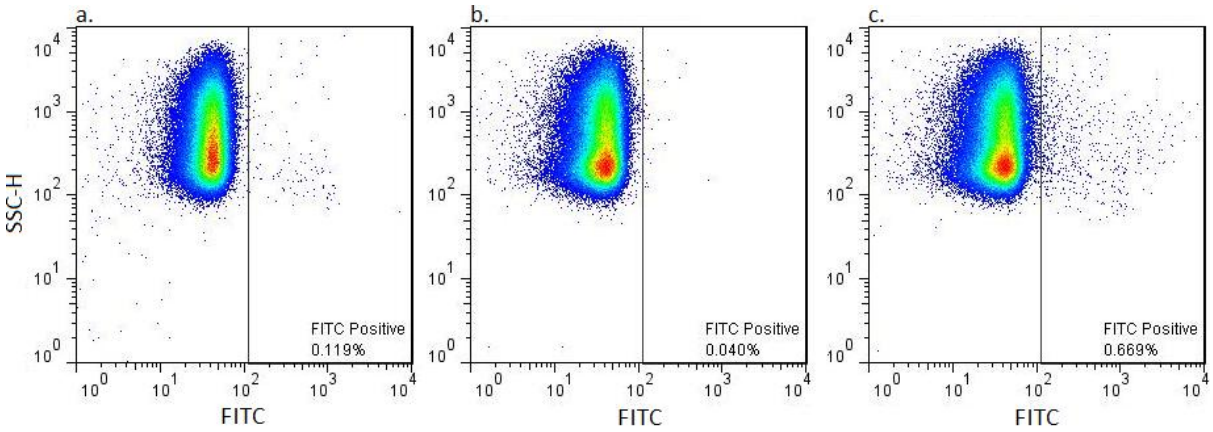

Fig. 3.24. Antibody specificity controls. (a) Uninfected erythrocytes: 1° anti-MSP-1 19 kDa and 2° antibody (negative control). (b) Peruvian isolate 3541 containing 2% schizonts: 2° antibody only (negative control). (c) Peruvian isolate 3541 containing 2% schizonts: 1° anti-MSP-1 19 kDa and 2° antibody (positive control).

Permeabilised Peruvian isolate 3541 at a parasitaemia of 2% schizonts exhibited higher levels of anti-MSP-1 19 kDa antibody binding (FITC positive, 0.67%; Fig. 3.24 c) than the negative controls of uninfected erythrocytes (FITC positive, 0.12%; Fig. 3.24 a) or 2% schizonts from Peruvian isolate 3541 with only secondary antibody (FITC positive, 0.04%; Fig. 3.24 b). This control showed that the 1° antibody binds specifically to MSP-1 and not to uninfected erythrocytes, and that there was no non-specific binding of the 2° antibody.

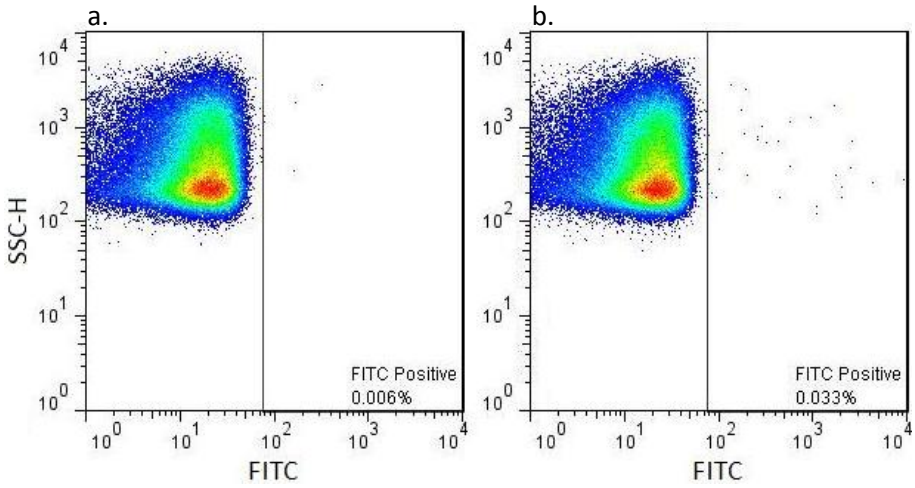

Fig. 3.25. Peruvian isolate 3541 at a parasitaemia of 6% rings. (a) 2° antibody only (negative control). (b) 1° anti-MSP-1 19 kDa antibody and 2° antibody (negative control).

Peruvian isolate 3541 at a parasitaemia of 6% rings was used as a negative control to show that there was no extracellular MSP-1 present in isolates lacking the intermediate population (Fig. 3.25). No MSP-1 and associated merozoites were detected with 1° anti-MSP-1 19 kDa antibody and FITC conjugated 2° antibody (Fig. 3.25 b), compared to 2° antibody used alone (Fig. 3.25 a).

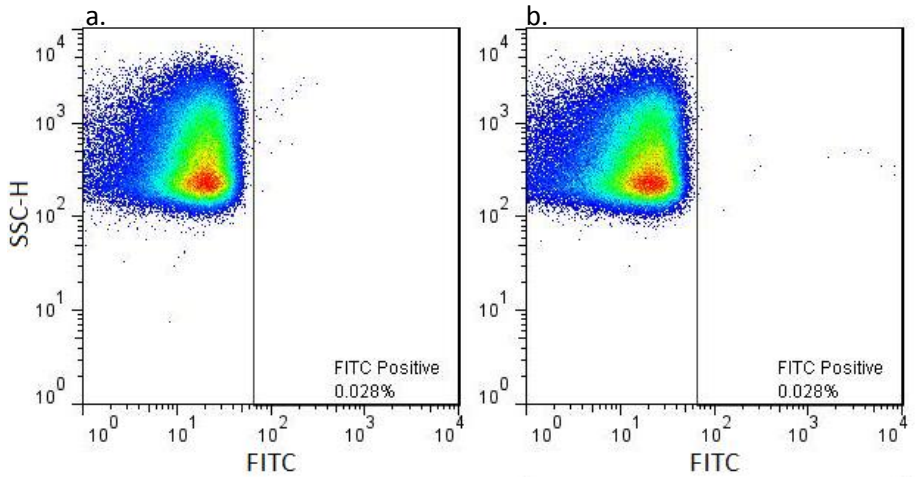

Fig. 3.26. Peruvian isolate 3769 at a parasitaemia of 6% rings. (a) 2° antibody only (negative control). (b) 1° anti-MSP-1 19 kDa antibody and 2° antibody.

Peruvian isolate 3769 contained the intermediate population hypothesised to be caused by merozoite adherence. However, no extracellular MSP-1 specific labelling was detected on this isolate (Fig. 3.26b).